Recruitment of endocytosis in sonopermeabilization-mediated drug delivery: A real-time study

Marc Derieppe, Katarzyna Rojek, Jean-Michel Escoffre, Baudouin Denis de Senneville, Chrit T. W. Moonen, Clemens Bos

Recruitment of Endocytosis in Sonopermeabilization-mediated Drug Delivery: a Real-Time Study

Marc Derieppe[1¶*], Katarzyna Rojek[1,2¶], Jean-Michel Escoffre[1], Baudouin Denis de Senneville[1,3], Chrit Moonen[1], Clemens Bos[1]

[1]Imaging Division, University Medical Center Utrecht, Utrecht, Netherlands

[2] Present address: Laboratory of Synaptogenesis, Cell Biology Department, Nencki Institute of Experimental Biology, Polish Academy of Sciences, Warsaw, Poland

[3]Institut de Mathématiques de Bordeaux, UMR 5251 CNRS, Université Bordeaux 1, INRIA, Bordeaux, France

[¶] The authors contributed equally to this work.

* Corresponding author

Email : m.derieppe@umcutrecht.nl (MD)

Abstract

Microbubbles (MB) in combination with ultrasound (US) can enhance cell membrane permeability, and have the potential to facilitate the cellular uptake of hydrophilic molecules. However, the exact mechanism behind US- and MB-mediated intracellular delivery still remains to be fully understood. Among the proposed mechanisms are formation of transient pores and endocytosis stimulation. In our study, we investigated whether endocytosis is involved in US- and MB- mediated delivery of small molecules.

Dynamic fluorescence microscopy was used to investigate the effects of endocytosis inhibitors on the pharmacokinetic parameters of US- and MB-mediated uptake of SYTOX Green, a 600 Da hydrophilic model drug. C6 rat glioma cells, together with SonoVue® microbubbles, were exposed to 1.4 MHz ultrasound waves at 0.2 MPa peak-negative pressure. Collection of the signal intensity in each individual nucleus was monitored during and after US exposure by a fibered confocal fluorescence microscope designed for real-time imaging.

Exposed to ultrasound waves, C6 cells pretreated with chlorpromazine, an inhibitor of clathrin-mediated endocytosis, showed up to a 2.5-fold significant increase of the uptake time constant, and a 1.1-fold increase with genistein, an inhibitor of caveolae-mediated endocytosis. Both inhibitors slowed down the US-mediated uptake of SYTOX Green.

With C6 cells and our experimental settings, these quantitative data indicate that endocytosis plays a role in sonopermeabilization-mediated delivery of small molecules with a more predominant contribution of clathrin-mediated endocytosis.

Introduction

In oncology, microbubble-assisted ultrasound was introduced as a promising method to improve therapeutic efficacy of drugs by increasing their local delivery. In the presence of microbubbles, tissue exposure to ultrasound waves transiently increases the permeability of biological barriers, such as cell membranes to increase the intracellular uptake of drugs, and blood vessels to enhance drug extravasation [1-3]. This technology is especially exploited to circumvent poor transendothelial transport, and transmembrane transport of hydrophilic anticancer drugs, such as DNA intercalating agents, *i.e.* gemcitabine [4] or irinotecan [5]. The potential of this approach for cancer therapy is clearly shown in an increasing number of publications on preclinical [6-9] and clinical [4] drug delivery using microbubble-assisted ultrasound.

Many studies have found that US-mediated plasma membrane permeabilization results from the formation of transient pore-like structures in the plasma membrane, thus facilitating the delivery of molecules of different molecular weights into the intracellular compartment [10-12]. Hence, this phenomenon was named sonoporation [13]. The cause of these transient structures in the plasma membrane is commonly assumed to be acoustic cavitation [10]. The use of ultrasound contrast agents (*i.e.* gaseous microbubbles) may enhance this effect by initiating the nucleation of the cavitation [14] in this vicinity, and reduces the required energy deposition in the tissues during US exposure. Cavitation can be categorized either as 1) inertial cavitation, which involves rapid growth and collapse of MBs [14], or as 2) stable cavitation with an oscillatory motion of bubbles with fluid microstreamings exerting shear forces on the plasma membrane [14]. Both induce transient and local cell membrane permeabilization. At the single-cell level, microbubbles were reported to exhibit a

sonopermeabilization when the distance between the microbubble shell and the plasma membrane equals at most three times the microbubble diameter [15]. Therefore, sonopermeabilization protocols consist of mixing microbubbles with cells *in vitro*, or *in vivo* injecting them intravascularly or intratumorally to ensure the close vicinity of microbubbles with endothelial and tumor cells.

However, there is increasing evidence that cavitation-mediated mechanical stimuli induce the recruitment of endocytosis in US and MB-mediated drug [16-17] and gene delivery [18-19]. Using endocytosis inhibitors, such as chlorpromazine [17] and genistein [20], previous studies [18] showed that clathrin- and caveolae-mediated pathways were recruited for the US-mediated intracellular delivery of macromolecules, such as dextran from 4.4 to 500 kDa. Other studies suggested a selective contribution of one of the two endocytosis pathways: clathrin-mediated endocytosis has been proposed to facilitate the internalization of plasmid DNA [21] whereas caveolae-mediated endocytosis has been suggested to promote the delivery of fluorescently tagged proteins into endothelial cells [22]. However, to our knowledge, few studies providing real-time quantitative information of model drug uptake upon ultrasound exposure has been conducted yet at the single-cell level [23] and in a cell population [24].

Previously, we showed that the real-time monitoring of the uptake of SYTOX Green model drug upon US exposure was feasible using a dedicated setup incorporating a fibered confocal fluorescence microscope (FCFM) [24]. From the image sequence displaying the fluorescence signal enhancement of a cell population of more than a hundred of cells, the pharmacokinetic parameters of each cell were accurately assessed by implementing a complete post-processing pipeline, which was automated from the data preprocessing to the statistical analysis of the population kinetic data [25]. We used SYTOX Green intercalating dye, which is cell impermeable and exhibits fluorescence intensity upon binding to nucleic

acids, making it a probe of plasma membrane permeabilization [26]. We tested the hypothesis that endocytosis was recruited for US-mediated intracellular delivery of 600 Da SYTOX Green model drug. Specifically, we investigated the effect of endocytosis inhibitors on the pharmacokinetic parameters derived from the real-time monitoring of SYTOX Green uptake [24].

Materials and Methods

Cell culture

C6 rat glioma cells (ATCC® number: CCL-107™) were grown as a monolayer in Dulbecco's modified Eagle's medium (DMEM, Sigma-Aldrich®, St. Louis, MO) with low glucose concentration (1 g/L) and stable glutamine supplemented with 10% fetal bovine serum (Sigma-Aldrich®) and 1% penicillin-streptomycin (Sigma-Aldrich®). The cells were routinely subcultured every 4 days and incubated at 37°C in humidified atmosphere with a 5% CO_2 incubator. This cell line is frequently used to develop and optimize sonopermeabilization for drug and gene delivery [27-29].

Endocytosis inhibitors

Cells were incubated in the presence of two endocytosis inhibitors: 1) Chlorpromazine (Sigma-Aldrich®), an inhibitor of clathrin-mediated endocytosis, from 10 µM to 60 µM. Chlorpromazine translocates clathrin together with its adapter protein from the plasma membrane to intracellular vesicles, thus hindering the formation of clathrin-coated pits at the cell surface [30]; 2) Genistein (Sigma-Aldrich®), an inhibitor of caveolae-mediated endocytosis from 200 µM, typical minimum concentration for efficient and non toxic effect of genistein for C6 cells [31], to 300 µM. Genistein hinders caveolae-coated vesicle internalization by blocking dynamin-2 ring assembly, which is critical for late stages of membrane invagination [32].

Selection of the inhibitor concentration – cell viability assessment

XTT assays, which are based on metabolic turnover of tetrazolium dye by living cells, were performed to determine a concentration range of chlorpromazine and genistein to study their effect while limiting their cytotoxicity. Neither ultrasound waves nor microbubbles have been used in these assays. 5×10^3 cells/well were seeded in a 96-well plate for 20 hours and subsequently incubated at 37 ºC and 5 % CO_2 with complete DMEM medium containing either 50-300 µM genistein, or 10-100 µM chlorpromazine for 30 minutes (min). After incubation, 50 µL XTT solution (XTT Cell Proliferation Assay Kit - ATCC®, Netherlands) was added to each well, which was prepared by adding 100 µL solution of 1-methoxy phenazine methosulfate to 5 mL of XTT. Cells were then further incubated at 37ºC, 5% CO_2 for 1 hour. The absorbance of colored formazans was measured at 492 nm using an EZ Read 400 Microplate reader (Biochrom, Cambridge, United Kingdom), and corrected for the reference absorbance at 620 nm. Measured absorbance values were normalized by the absorbance without inhibitor. All tests were performed at least in quadruplicate. Subsequently, the influence of the incubation time in the presence of the inhibitor was evaluated by assessing the cytotoxicity at 0.5, 1.5 and 3 hours of incubation with the selected inhibitor concentrations. These incubation times were chosen based on the expected duration of the FCFM experiment. Results were presented as mean ± standard error of the mean (SEM).

Sensitivity and specificity of the inhibitors

Sensitivity and specificity of chlorpromazine and genistein endocytosis inhibitors were evaluated by staining clathrin and caveolae vesicles with 50 µg/mL Human transferrin (HTr) – Alexa Fluor 488 nm conjugate (Sigma-Aldrich®) and 10 µg/mL Cholera Toxin (Chol Tox) –

Alexa Fluor 488 nm conjugate (Sigma-Aldrich®), respectively. Here, neither ultrasound waves nor microbubbles have been used in this evaluation. First, C6 cells were seeded in µ-slide 4 well glass bottom chamber (ibidi GmbH, Germany) for 3 days and reached 90 % confluency at the day of the experiment (7×10^4 cells/well). The cells were once washed with Phosphate Buffer Saline (PBS) and their medium was changed to cell culture medium without serum. After inhibitor addition, the cells were further incubated for 30 min at 37 ºC and 5 % CO_2. Subsequently, HTr or Chol Tox was added and the cells were incubated with the inhibitor and the marker for 1 hour. For cell viability assessment, propidium iodide (PI) at 0.1 µg/mL was added to the cells, followed by incubation for 10 min. The medium was then removed, and the cells were thrice washed with PBS with Ca^{2+} and Mg^{2+}. Finally, cells were fixed for 20 min using 4% paraformaldehyde in PBS, and stored in PBS with Ca^{2+} and Mg^{2+}. Fluorescence images of the endocytosis vesicles were collected with a laser scanning confocal fluorescence microscope (LSM 700, AxioObserver, Carl Zeiss Microscopy GmbH, Jena, Germany) and a Plan-Apochromat 63x oil-immersion objective, 1.4 numerical aperture, 488 nm and 555 nm excitation wavelengths, a 0.1 µm numerical spatial resolution, and a 1024×1024-pixel matrix.

Assessment of the uptake kinetics in the presence of the endocytosis inhibitors – Real-time imaging

Real-time monitoring of the US-mediated model drug uptake was based on the use of SYTOX Green intercalating fluorescent dye (Life Technologies™, Saint-Aubin, France) (Excitation 504 nm / Emission 523 nm) [24]. This small molecular-weight (600 Da) fluorescent dye is cell-impermeable, and exhibits a 100- to 1000- fold increase in fluorescence upon binding to

nucleic acids [33], thus making it a probe for US-mediated cell plasma membrane uptake [34].

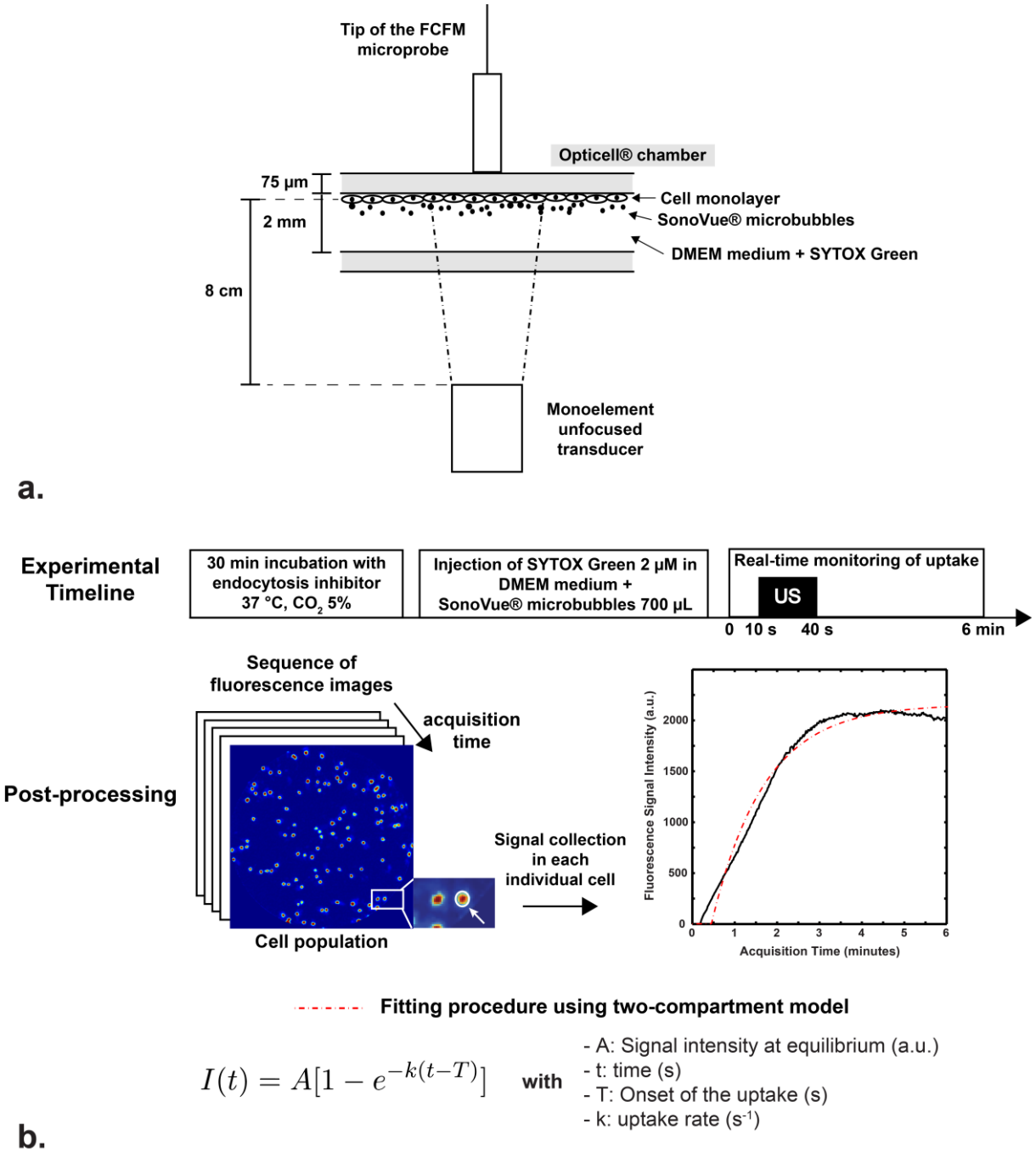

Figure 1. *In vitro* setup (a), timeline of the experiment (b – upper panel) and image post-processing (c – lower panel) for monitoring of ultrasound (US)- and microbubble-mediated cell uptake using fibered confocal fluorescence microscopy (FCFM).

As previously described, OptiCell™ culture chambers (Thermo Fischer Scientific, Rochester, NY, USA) were seeded with 4×10^6 cells 48 hours prior to the experiment. C6 cells grow as an adherent monolayer in this culture chamber, favoring the contact between the microbubbles and the plasma membranes of the cell monolayer. Using SYTOX Green model drug and this culture chamber, paracellular transports are outside the scope of this study. On the day of the experiment, cells displayed 80 – 90 % confluence and were provided with fresh complete DMEM medium. Then, cells were exposed to the inhibitor for 30 min at 37 ºC, 5% CO_2, but also during the subsequent imaging session lasting between 1 hour and 2.5 hours. In the presence of the endocytosis inhibitors, the impact of this incubation time on the uptake kinetics was evaluated, and showed no significant difference (Kruskall-Wallis test, $p > 0.05$) (data not shown). Subsequently, SYTOX Green at a final concentration of 2 µM and a commercially available ultrasound contrast agent (SonoVue®, Bracco, Milan, Italy) at a ratio of 20 microbubbles per cell were added to the cell culture chamber. The OptiCell™ wall containing the cell monolayer was placed upwards to favor contacts between the cell monolayer and the microbubbles subjected to the buoyancy. The US setup consisted of a 20 mm-diameter unfocused mono-element US transducer (Precision Acoustics, Dorchester, UK) positioned 8 cm below the OptiCell™ cell-culture chamber (Figure 1a). Cells were exposed to US waves for 30 s, with the following settings: 1.4 MHz central frequency, 10% duty cycle with 1 kHz pulse repetition frequency to trigger microbubble cavitation, 0.2 MPa peak negative acoustic pressure yielding a low mechanical index of 0.2 suitable for drug delivery. As reported previously [35], the two OptiCell™ membranes attenuated less than 2 % of the energy of the US beam. According to the short echo train of the pulse, the water surface was 10 cm above the OptiCell™ to prevent the buildup of standing waves. Generating only stable cavitation, these acoustic parameters have been optimized to induce an efficient and transient membrane permeabilization while limiting cell detachment and cell mortality (unpublished

data). To choose the central frequency, a compromise has been made between the highest acoustic yield of the transducer, *i.e.* 1.4 MHz, and the absorption peak of the SonoVue® microbubbles at the sub-harmonic frequency, *i.e.* 1.7 MHz [36]. Fibered Confocal Fluorescence Microscopy (FCFM, CellVizio®, Mauna Kea Technologies, Paris, France) was conducted with an excitation wavelength of 488 nm. Imaging sequences were collected during 6 minutes at 8.5 frames per second, with the 30 s sonication starting after 10 s of imaging (Figure 1b). The fluorescence images were acquired at a working distance of 100 µm, a lateral resolution of 3.9 µm and a field of view of 593×593 µm. For each inhibitor concentration, the experiment was performed at least in triplicate. Each imaging session started with a control experiment, in which cells were not subjected to any endocytosis inhibitor.

Data analysis

Uptake kinetics of SYTOX Green were obtained from the real-time fluorescence data as described in [25]. The cell nuclei were detected using the Radial-Symmetry-Transform (RST) algorithm [37], and tracked frame-by-frame using an Iterative-Closest-Point (ICP) algorithm [25]. The fluorescence signal intensity profiles were then analyzed for each nucleus individually (Figure 1b). A two-compartment model was proposed to represent the extracellular space and the intracellular compartment, separated by a plasma membrane. This model neglected the diffusion of SYTOX Green in the cytoplasm and the crossing of the nuclear membrane, as previous studies indicated that these two steps were extremely rapid for molecules with a molecular weight lower than 5 kDa [38-39]. The corresponding signal intensity *(I)* is as follows:

$$I(t) = A\,[1 - \exp(-k(t-T))],$$

where A is the asymptotic signal enhancement, T the time of signal onset, and k the uptake rate. The model was considered accurate when Pearson's correlation coefficient (r^2) was greater than 0.95; the values of the uptake rate of SYTOX Green were reported as median with interquartile ranges.

The statistical analysis was performed using GraphPad Prism software (La Jolla, CA, USA). To evaluate the viability of C6 cells preincubated during 30 min, each cell population exposed to a concentration of endocytosis inhibitor was compared to the one without endocytosis inhibitor, *i.e.* the reference population, using the unpaired non-parametric Mann-Whitney test (MW), as the values of viability in the cell populations were not distributed normally. The effect of the incubation time on cell viability was tested using the unpaired non-parametric Kruskall-Wallis test (KW). The distributions of time constants obtained from two inhibitor concentrations were compared using the MW test. For all the tests, the results were considered significant when p was lower than 0.05.

Results derived from control experiments were collected until the end of the study and two separate control data sets were created. In the first set, we accumulated all control data for genistein, *i.e.,* all control data from the same days when the different concentrations of genistein (200, 250 and 300 μM) were tested. The second consisted of all control data for chlorpromazine. For each inhibitor concentration, FCFM experiments were performed at least three times.

Results

Selection of the inhibitor concentration – cell viability assessment

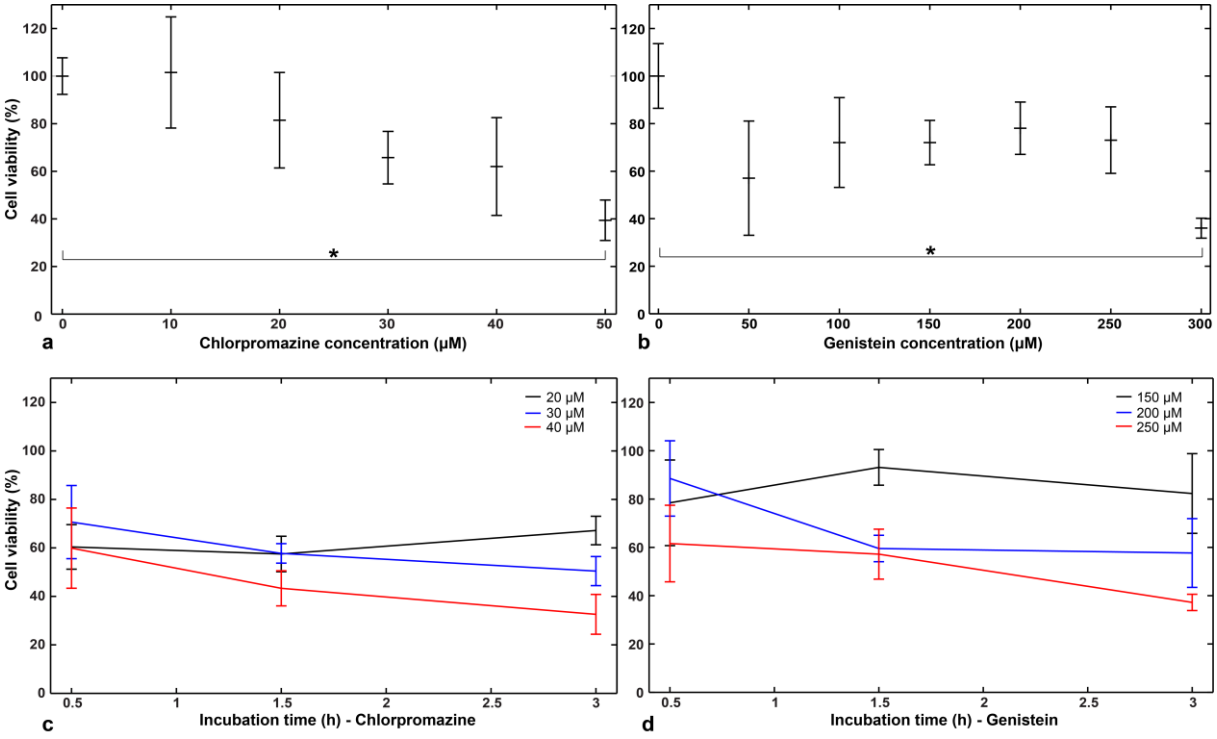

Figure 2. Effect of the endocytosis inhibitors on cell viability (*p < 0.05). C6 cells were incubated for 30 minutes at different concentrations of chlorpromazine (a) and genistein (b). Subsequently, the influence of the incubation time in the presence of chlorpromazine (c) and genistein (d) was evaluated from 0.5 hours to 3 hours. Results: Mean ± SEM; n ≥ 4.

At high concentrations, both endocytosis inhibitors have an effect on the viability of C6 cells, which were for these experiments not exposed to US and microbubbles. According to the XTT absorbance data, a loss of cell viability was noticed from 20 µM of chlorpromazine, followed by a continuous decrease, until reaching a significant loss below 50 % at 50 µM (MW, $p < 0.05$) (Figure 2a). Conversely, cell viability was not affected by genistein in a dose-dependent manner: a plateau of 70 % viability was observed until a significant decrease of viability at 300 µM of genistein (MW, $p < 0.05$) (Figure 2b).

The influence of the incubation time on cell viability was evaluated at 0.5, 1.5 and 3 hours of incubations with concentrations of chlorpromazine (Figure 2c) and genistein (Figure 2d) for which cell viability was over 50 %. The cytotoxic effect of 20 µM chlorpromazine is relatively stable and was approximately 60 % from 0.5 to 3 hours of incubation time. For higher chlorpromazine concentrations, the cell viability decreased by 10 to 20 % when the incubation time extended to 1.5 and 3 hours. No significant difference was found in each of the 3 concentrations (KW, $p > 0.05$). Concerning genistein, an effect of the incubation time on cell viability was observed for concentrations above 200 µM, with a non-significant decrease of cell viability of up to a 20 to 30 % with an incubation time of 3 hours (KW, $p > 0.05$). These data suggest that the cytotoxicity variations are acceptable in the presence of chlorpromazine or genistein during the time needed to perform the FCFM session.

Inhibition specificity and cell sensitivity

The sensitivity of C6 cells to the inhibitors, in the absence of ultrasound and microbubbles, was determined by staining clathrin and caveolae vesicles, and observing cell morphology by laser scanning confocal microscopy. Without inhibitor, cells showed an elongated cytoplasm (Figure 3a), which is typical of glial cells, indicating integrity of the cytoskeleton. The absence of PI signal in the nucleus indicated that cell plasma membranes are intact (Figure 3b). Stained with human transferrin with Alexa Fluor 488 conjugate, punctiform clathrin vesicles were distributed in the cytoplasm. As CTZ concentration increased, C6 glioma cells first lost their elongated shape, which would suggest that cytoskeleton activity is hampered at this concentration (Figure 3d,g). However, the distribution of stained clathrin vesicles remained apparently homogeneous in the cytoplasm. At 40 µM (Figure 3j), the absence of elongated cytoskeleton was also observable, and clathrin vesicles are predominantly located at the plasma membranes, according to the high fluorescence signal densely expressed at this

site, also observed in Vercauteren *et al.* [32]. This suggests that chlorpromazine indeed impedes clathrin-mediated transport. At 50 μM of chlorpromazine (Figure 3m), only a diffuse background fluorescence was noticed in cell cytoplasm with few vesicles. At this concentration, PI fluorescence signal is present at the nucleus, indicating that chlorpromazine affected the integrity of the plasma membranes (Figure 3n).

Moreover, the specificity of chlorpromazine specificity was verified by exposing cells whose caveolae vesicles were stained with Cholera Toxin – Alexa Fluor 488 conjugate to the clathrin-vesicle inhibitor (Figure S1d,g,j,m). From 20 to 40 μM of chlorpromazine, caveolae vesicles stained with Cholera toxin were distributed homogeneously in the cytoplasm, suggesting that chlorpromazine did not impede trafficking of caveolae vesicles (Figure S1d,g,j). Again, cells exposed to chlorpromazine at 50 μM showed a diffuse background signal with PI signal present in the nuclei, suggesting that the integrity of plasma membrane was affected (Figure S1n).

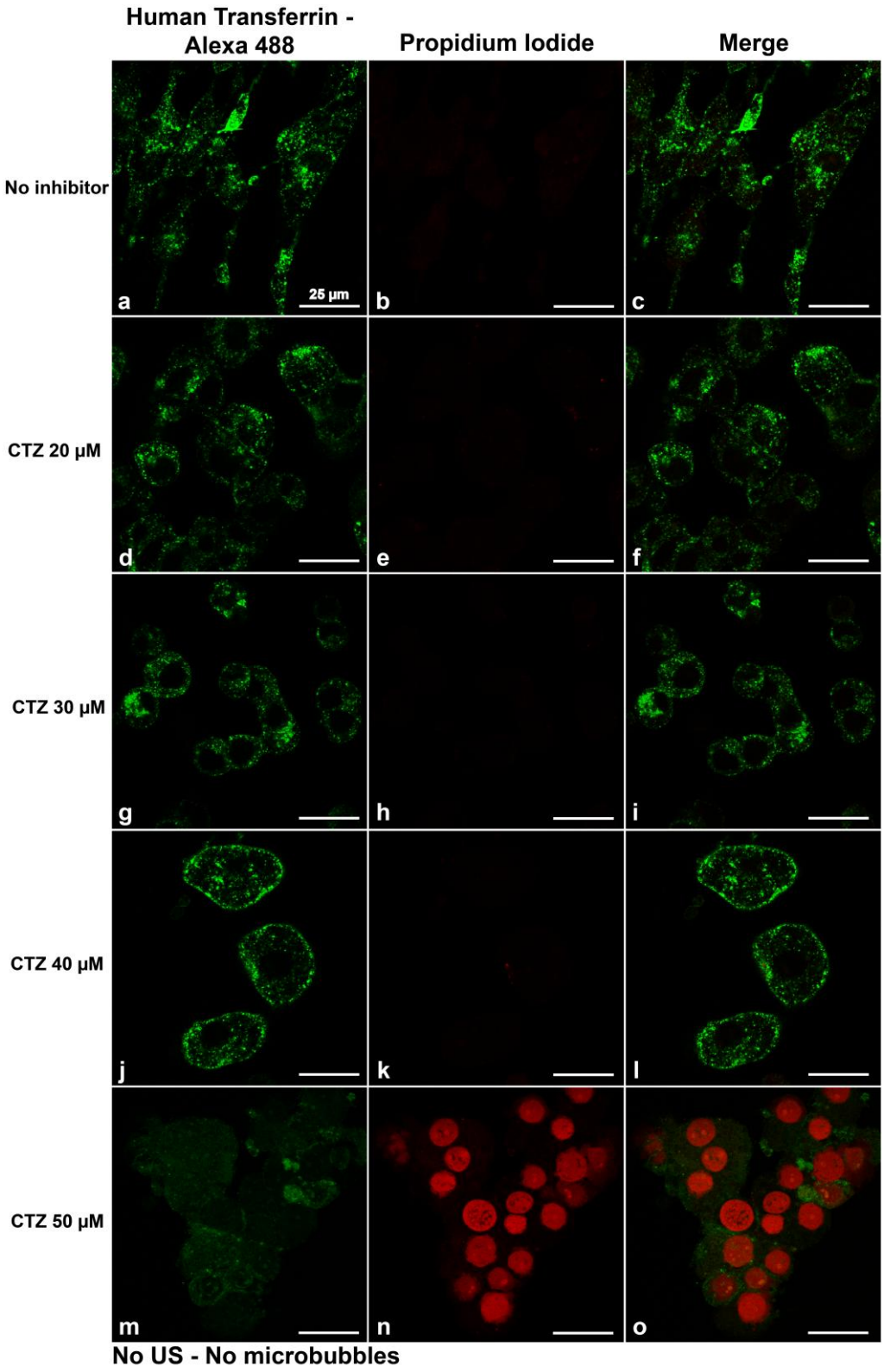

Figure 3. **Sensitivity experiment – Effect of chlorpromazine (CTZ) from 0 µM to 50 µM on clathrin vesicles** (green channel: human transferrin – Alexa Fluor 488 nm conjugate) (a,d,g,j,m). The integrity of cell plasma membrane is evaluated using Propidium Iodide (PI – red channel) (b,e,h,k,n). Bar: 25 µm.

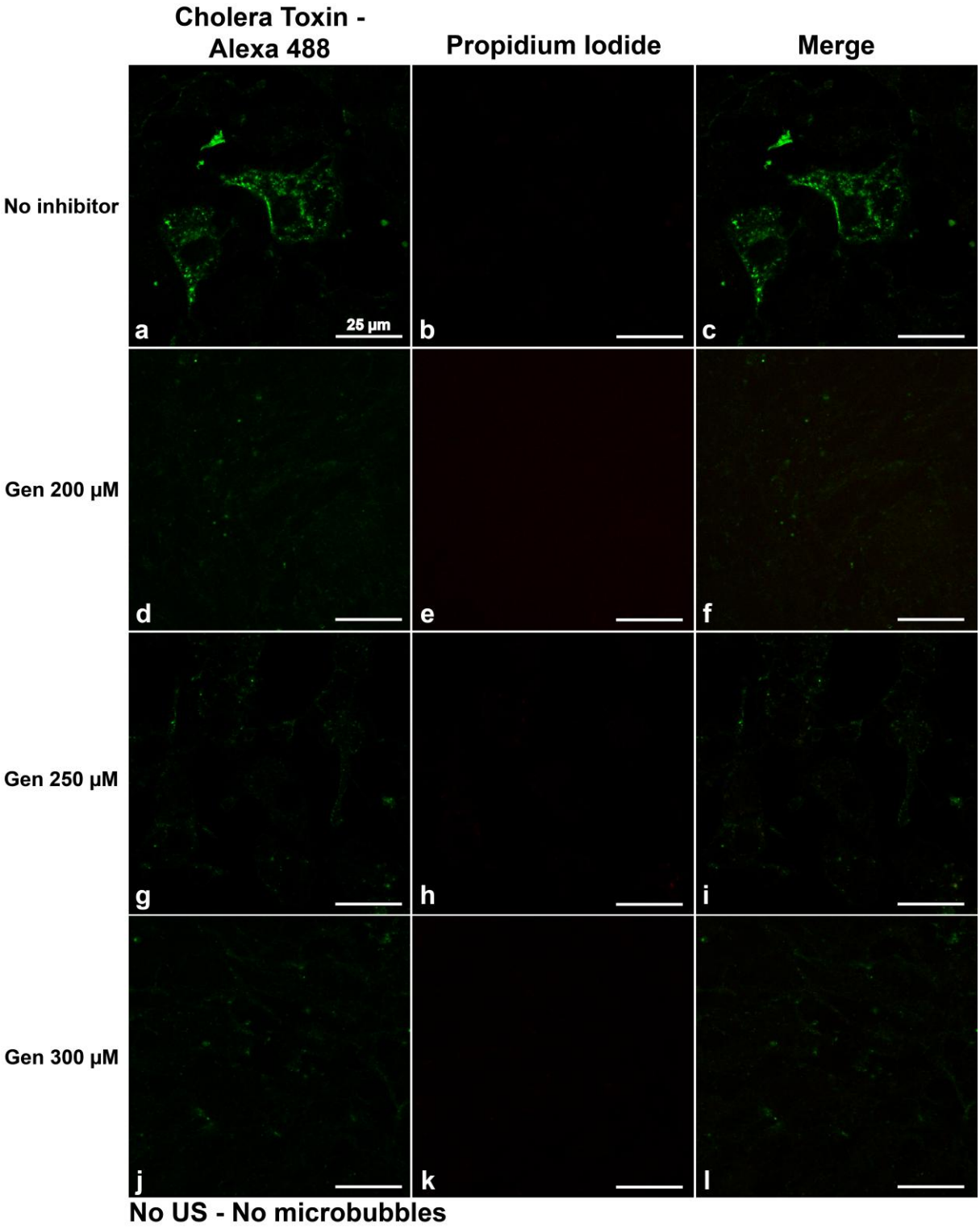

Figure 4. Sensitivity experiment – Effect of genistein (Gen) from 0 µM to 300 µM on caveolae vesicles (green channel: Cholera Toxin – Alexa Fluor 488 nm conjugate) (a,d,g,j). Cell plasma membrane integrity is evaluated using Propidium Iodide (PI – red channel) (b,e,h,k). Bar: 25 µm.

In the presence of genistein from 200 to 300 µM, staining of caveolae vesicles with Cholera Toxin – Alexa Fluor 488 conjugate showed an acute inhibition of caveolae-mediated pathway in the cytoplasm (Figure 4d,g,j), according to the low number of caveolae vesicles in the cytoplasm compared to the control without inhibitor. No PI fluorescence signal is present in cell nuclei, suggesting good cell integrity (Figure 4b,e,h,k).

Conversely, staining of clathrin vesicles showed images in the presence of genistein from 200 to 300 µM comparable to the images without inhibitor (Figure S2d,g,j), with punctiform structures homogeneously distributed in the cytoplasm. Here, the elongated shape of the plasma membranes confirms the integrity of the cytoskeleton, also suggested by the absence of PI fluorescence signal in the nuclei. Thus, genistein did not inhibit clathrin-mediated pathway in the range of concentrations investigated here. In the scope of our study, genistein and chlorpromazine can therefore be considered specific and effective inhibitors of endocytosis in C6 cells.

Assessment of the uptake kinetics in the presence of the endocytosis inhibitors – Real-time imaging

In a sonopermeabilization experiment, C6 cells exposed to genistein showed a statistically significant but modest (MW, $p < 0.05$) increase of the uptake time constant $1/k$ of SYTOX Green, from 52 s (20 s, n = 451) without inhibitor to 58 s (22 s, n = 352) at 300 µM of genistein, respectively (Figure 5 and S3a,c). Also, time-constant differences between 200 µM and 250 µM, and between 200 µM and 300 µM of genistein were statistically significant (MW, $p < 0.05$). These data suggest that caveolae-mediated pathway has a low recruitment level during sonopermeabilization-stimulated uptake for this cell line and our US settings.

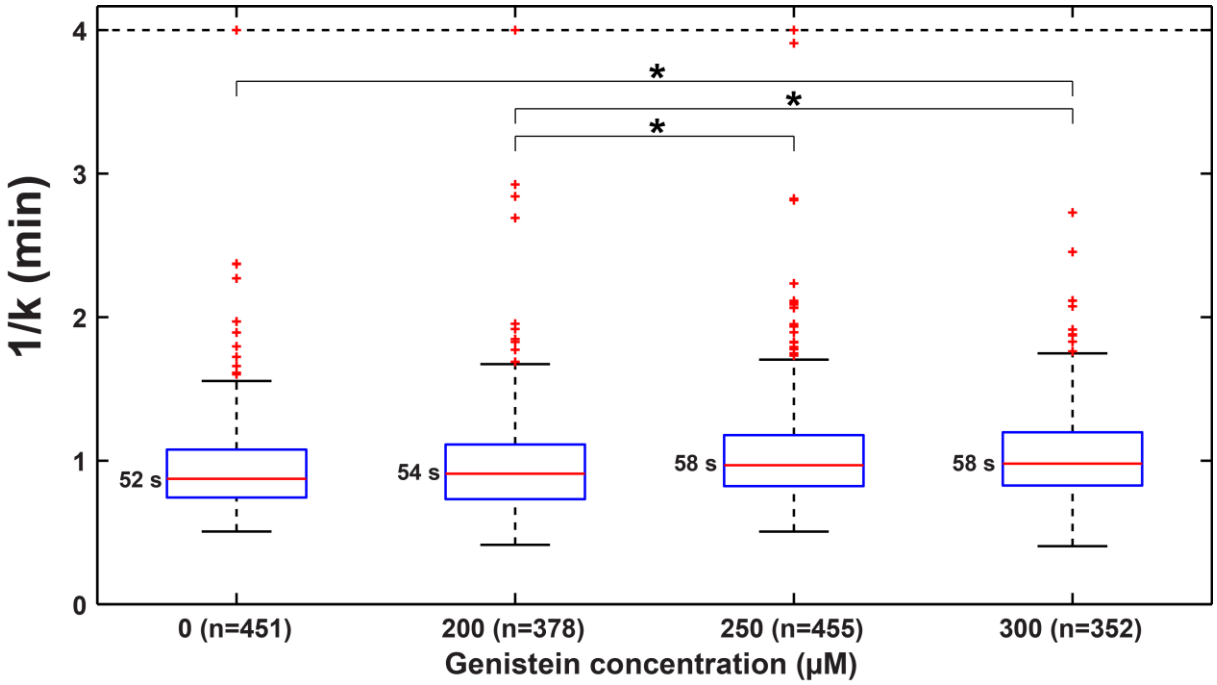

Figure 5. Effect of genistein, caveolae inhibitor, on the uptake time constants 1/k of SYTOX Green model drug (*$p < 0.05$). Exposed to 1.4 MHz ultrasound waves (mechanical index: 0.2) and SonoVue® microbubbles, C6 cells display a statistically significant but modest increase of the uptake time constants $1/k$ in the presence of genistein.

Cells in the presence of chlorpromazine showed a dose-dependent slowing down of SYTOX Green uptake from 52 s (22 s, n = 946) without treatment to 2 min 11 s (1 min 33 s, n = 262) at 40 µM of chlorpromazine, respectively (Figure 6 and S3b,c). All distributions from 0 µM to 50 µM were significantly different from others (MW, $p < 0.05$).

This dose-dependent response, where chlorpromazine led to slower intracellular transport of SYTOX Green, indicated hindrance of the clathrin-mediated pathway. As a corollary, these results imply the contribution of the clathrin-mediated pathway in the US-mediated uptake of SYTOX Green model drug. In addition, the increase of the time constants was larger for the inhibition of the clathrin-mediated pathway than for the inhibition of the caveolae-mediated pathway. Therefore, we infer that microbubble-assisted ultrasound primarily recruited the clathrin-mediated pathway.

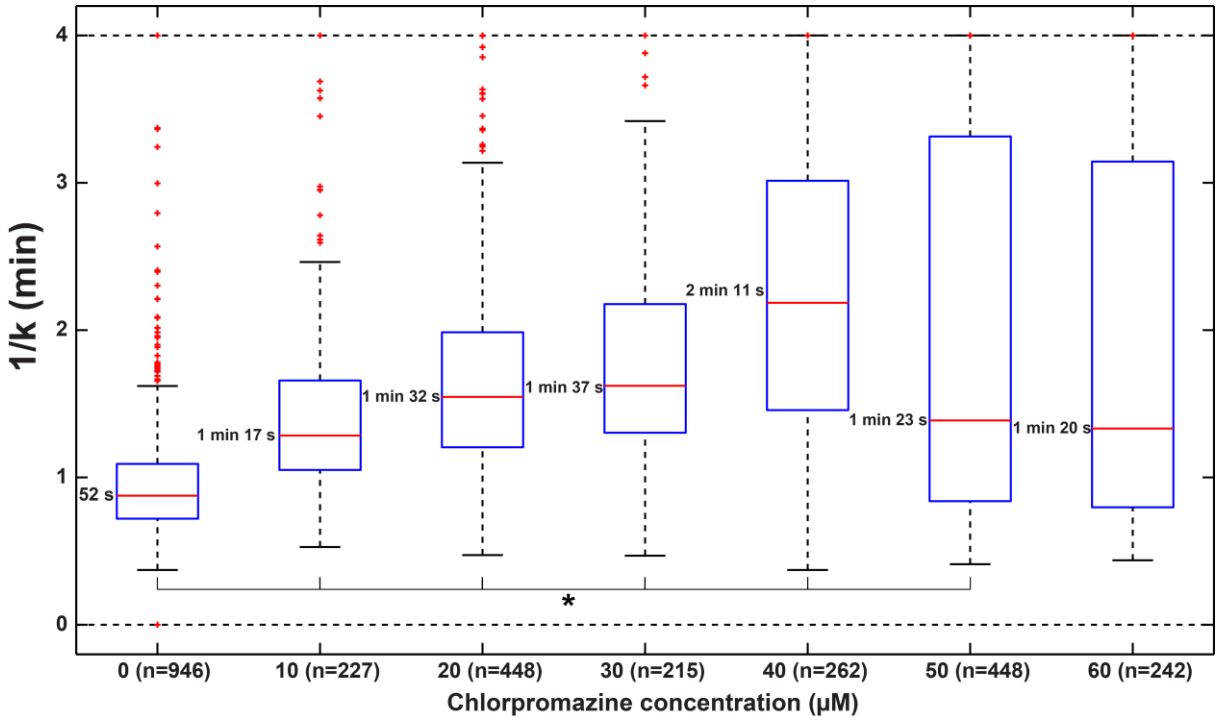

Figure 6. Effect of chlorpromazine, clathrin inhibitor, on the uptake time constants, 1/k of SYTOX Green (*$p < 0.05$). C6 cells in the presence of chlorpromazine showed a dose-dependent slowing down of SYTOX Green uptake. All distributions from 0 µM to 50 µM were significantly different from others. At 50 µM and 60 µM of chlorpromazine, an abrupt decrease of the time constant $1/k$ was observed. This suggests a loss of cell membrane integrity, as was observed with the confocal images.

An abrupt decrease of the time constant $1/k$ was observed with chlorpromazine concentrations at 50 µM and 60 µM (Figure 6). The rapid sonopermeabilization-mediated uptake suggests a loss of cell membrane integrity, as also observed with the confocal images: 1 min 23 s (2 min 28 s, n=448) at 50 µM, and 1 min 20 s (2 min 21 s, n=242), at 60 µM. These time constants were not significantly different for these concentrations (MW, $p = 0.54$).

Discussion

A better understanding of sonopermeabilization bioeffects on tumor cell plasma membranes is required to potentially optimize delivery of poorly permeable anticancer agents. Here, we demonstrated the recruitment of endocytosis in sonopermeabilization-mediated delivery of small molecules (< 4 kDa), *in vitro*, using real-time fluorescence imaging. In C6 rat glioma cells, we derived pharmacokinetic parameters derived from the fluorescence signal enhancement of a cell population [25]. This automated approach allowed us to quantify the effect of two endocytosis inhibitors, *i.e.* chlorpromazine and genistein, on the US-mediated uptake kinetics of SYTOX Green model drug.

The real-time monitoring of the model drug uptake showed a relation between the uptake time constants and the inhibitor concentration in a dose-dependent manner. With a significant 2.5-fold increase of the uptake time constant, chlorpromazine was found to have a higher effect on the slowing down of SYTOX Green uptake kinetics than genistein, whose time constant displayed a 1.1-fold increase. This suggests a predominant role of the clathrin-mediated pathway in sonopermeabilization-mediated drug delivery. These data raise the question of the key factors determining the preferred route of cellular entry when cells are sonopermeabilized. Meijering *et al.* [17] showed that inhibition of clathrin-mediated endocytosis has a substantial effect on the cellular uptake of dextran macromolecules at different molecular weights (4.4-500 kDa), whereas the inhibition of caveolae-mediated endocytosis only affects internalization of larger molecules (155 and 500 kDa). Using a 600-Da model drug that is also found to be preferably taken up via the clathrin-mediated pathway, these findings would support the link between the molecular weight of the compound and its route of cellular entry. Conversely, using scanning electron microscopy, Zeghimi *et al.* [20] showed primarily the recruitment of the caveolae-mediated pathway when U-87 MG human glioblastoma cells were exposed to US waves in presence of BR14® microbubbles. These

results indicate that there might be other factors than the molecular weight influencing the route of cellular entry during sonopermeabilization, like the cell line, the US parameters and the type of microbubbles. Here, we quantified the recruitment of endocytosis with C6 cells only and limited our experiments to ultrasound exposures using 1.4 MHz and 0.2 MPa peak negative acoustic pressure, frequently used settings in sonopermeabilization studies. However, in US- and microbubble-mediated sonopermeabilization, acoustic pressure and frequency may have an impact on the nature of the internalization mechanism. These parameters may help optimize US- and microbubble-enhanced drug delivery, and should be considered in further investigations.

As shown by Vercauteren *et al.* [32], the cytotoxicity of endocytosis inhibitors is cell line dependent, thus requiring a study of the viability of C6 cells preincubated with the endocytosis inhibitors. A cell viability higher than 50 % could be found for chlorpromazine concentrations from 10 µM to 40 µM, and concentrations from 200 µM to 250 µM of genistein. Using laser scanning confocal microscopy, potential cytotoxicity of 50 µM chlorpromazine was observed by the presence of PI fluorescence signal in the nuclei, thus indicating the loss of plasma membrane integrity. Quantitative evaluation showed that the C6 cells preincubated with 50 µM chlorpromazine displayed an abruptly accelerated uptake. Previous studies have shown that cells undergoing apoptosis might be permeable to small molecules, such as fluorescent dyes [40], providing a possible explanation of this rapid uptake due to the loss of plasma membrane integrity.

Our results provide a possible explanation for recent observations that cells may exhibit increased permeability for hours after sonopermeabilization [41]. In this scenario, pores are quickly resealed to maintain plasma membrane integrity, after which transport is continued by endocytosis recruitment.

The exact intracellular fate of the endocytic vesicles derived from US- and microbubble-induced cavitation is of interest. In this case, SYTOX Green is not free by diffusing in the cytoplasm, but is encapsulated in endocytic vesicles instead. However, it ultimately reaches the nucleus, and yields a fluorescence signal. Using high-resolution microscopy, further study investigating cell trafficking of these endocytic vesicles would help decipher these mechanisms.

Conclusion

We have established *in vitro* the effect of two endocytosis inhibitors, i.e. chlorpromazine and genistein, on the pharmacokinetic parameters of a model drug uptake assessed in cell populations. Our approach showed that cells pretreated with endocytosis inhibitors and subsequently exposed to US in a presence of MB display slower uptakes, with a significant 2.5-fold increase of the uptake time constants with chlorpromazine concentration from 0 μM to 40 μM, and a shallow but significant 1.1-fold increase of the uptake time constants with genistein from 0 μM to 300 μM. These quantitative results support the recruitment of predominantly clathrin-mediated endocytosis in sonopermeabilization.

Acknowledgements

This work was supported by Advanced ERC grant Sound Pharma – 268906 (CM). The authors are grateful to Joep van den Dikkenberg and Georgi Nadibaidze for their technical support (Pharmaceutical Sciences Institute, University of Utrecht, Utrecht, the Netherlands). The data acquired with the Zeiss LSM 700 confocal microscope have been collected at the Cell Microscopy Core, Department of Cell Biology, University Medical Center Utrecht, Utrecht, Netherlands; the authors especially thank Corlinda ten Brink for her technical support.

References

[1] Sheikov N, McDannold N, Vykhodtseva N, Jolesz F, and Hynynen K (2004) Cellular mechanisms of the blood-brain barrier opening induced by ultrasound in presence of microbubbles. Ultrasound Med. Biol. 30:979-989.

[2] Sheikov N, McDannold N, Jolesz F, Zhang YZ, Tam K, et al. (2006) Brain arterioles show more active vesicular transport of blood-borne tracer molecules than capillaries and venules after focused ultrasound-evoked opening of the blood-brain barrier. Ultrasound Med. Biol. 32:1399–1409.

[3] Sheikov N, McDannold N, Sharma S, and K. Hynynen (2008) Effect of Focused Ultrasound Applied With an Ultrasound Contrast Agent on the Tight Junctional Integrity of the Brain Microvascular Endothelium. Ultrasound Med. Biol. 34:1093–1104.

[4] Kotopoulis S, Dimcevski G, Gilja OH, Hoem D, Postema M (2013) Treatment of human pancreatic cancer using combined ultrasound, microbubbles, and gemcitabine: A clinical case study. Med. Phys. 40:072902.

[5] Escoffre JM, Novell A, Serrière S, Lecomte T and Bouakaz A (2013) Irinotecan Delivery by Microbubble-Assisted Ultrasound: In Vitro Validation and a Pilot Preclinical Study. Mol. Pharm. 10:2667-2675.

[6] Treat LH, McDannold N, Vykhodtseva N, Zhang Y, Tam K, et al. (2007) Targeted delivery of doxorubicin to the rat brain at therapeutic levels using MRI-guided focused ultrasound. Int. J. Cancer 121:901–907.

[7] Rapoport NY, Kennedy AM, Shea JE, Scaife CL and Nam KH (2009) Controlled and targeted tumor chemotherapy by ultrasound-activated nanoemulsions/microbubbles. J. Control. Release 138:268–276.

[8] Park EJ, Zhang YZ, Vykhodtseva N and McDannold N (2012) Ultrasound-mediated blood brain/blood-tumor barrier disruption improves outcomes with trastuzumab in a breast cancer brain metastasis model. J. Control. Release 163:277–284.

[9] Sasaki N, Kudo N, Nakamura K, Lim SY, Murakami M, et al. (2012) Activation of Microbubbles by Short-Pulsed Ultrasound Enhances the Cytotoxic Effect of Cis-Diamminedichloroplatinum (II) in a Canine Thyroid Adenocarcinoma Cell Line In Vitro. Ultrasound Med. Biol. 38:109–118.

[10] Mehier-Humbert S, Bettinger T, Yan F and Guy RH (2005) Plasma membrane poration induced by ultrasound exposure: implication for drug delivery. J. Control. Release 104:213–222.

[11] Van Wamel A, Kooiman K, Harteveld M, Emmer M, ten Cate FJ, et al. (2006) Vibrating microbubbles poking individual cells: Drug transfer into cells via sonoporation. J. Control. Release 112:149–155.

[12] Schlicher RK, Radhakrishna H, Tolentino TP, Apkarian RP, Zarnitsyn V, et al. (2006) Mechanism of intracellular delivery by acoustic cavitation. Ultrasound Med. Biol. 32:915–924.

[13] Miller DL, Pislaru SV and Greenleaf JF (2002) Sonoporation: Mechanical DNA Delivery by Ultrasonic Cavitation. Somat. Cell Mol. Genet. 27:115–134.

[14] Suslick KS (1988) Ultrasound: its chemical, physical, and biological effects. VCH Publishers, New York, NY, USA

[15] Zhou Y, Yang K, Cui J, Ye JY, and Deng CX (2012) Controlled permeation of cell membrane by single bubble acoustic cavitation. ," J. Control. Release 157:103–111.

[16] Afadzi M, Strand SP, Nilssen EA, Masoy SE, Johansen TF, et al. (2013) Mechanisms of the ultrasound-mediated intracellular delivery of liposomes and dextrans. IEEE Trans. Ultrason. Ferroelectr. Freq. Control. 60:21–33.

[17] Meijering BDM, Juffermans LJM, van Wamel A, Henning RH, Zuhorn IS, et al. (2009) Ultrasound and Microbubble-Targeted Delivery of Macromolecules Is Regulated by Induction of Endocytosis and Pore Formation. Circ. Res. 104:679–687.

[18] Lee JL, Lo CW, Inserra C, Béra JC and Chen WS (2014) Ultrasound Enhanced PEI-Mediated Gene Delivery Through Increasing the Intracellular Calcium Level and PKC-δ Protein Expression. Pharm. Res. 31:2354-2366

[19] Juffermans LJM, Meijering BDM, Henning RH and Deelman LE (2014) Ultrasound and Microbubble-Targeted Delivery of Small Interfering RNA Into Primary Endothelial Cells Is More Effective Than Delivery of Plasmid DNA. Ultrasound Med. Biol. 40:532–540.

[20] Zeghimi A, Escoffre JM, Bouakaz A (2013) Sonoporation, endocytosis and pore formation. 19th European Symposium on Ultrasound Contrast Imaging Rotterdam, The Netherlands.

[21] De Paula DMB, Valero-Lapchik VB, Paredes-Gamero EJ and Han SW (2011) Therapeutic ultrasound promotes plasmid DNA uptake by clathrin-mediated endocytosis. J. Gene Med. 13:392–401.

[22] Lionetti V, Fittipaldi A, Agostini S, Giacca M, Recchia FA, et al. (2009) Enhanced Caveolae-Mediated Endocytosis by Diagnostic Ultrasound In Vitro. Ultrasound Med. Biol. 35:136–143.

[23] Fan Z, Liu H, Mayer M, and Deng CX (2012) Spatiotemporally controlled single cell sonoporation. Proc Natl Acad Sci USA. 109:16486–16491.

[24] Derieppe M, Yudina A, Lepetit-Coiffé M, Denis de Senneville B, Bos C, et al. (2013) Real-Time Assessment of Ultrasound-Mediated Drug Delivery Using Fibered Confocal Fluorescence Microscopy. Mol. Imaging Biol. 15:3–11.

[25] Derieppe M, Denis de Senneville B, Kuijf H, Moonen C, Bos C (2014) Tracking of Cell Nuclei for Assessment of In Vitro Uptake Kinetics in Ultrasound-Mediated Drug Delivery Using Fibered Confocal Fluorescence Microscopy. Mol. Imaging Biol. 16:642-651.

[26] Lepetit-Coiffé M, Yudina A, Poujol C, de Oliveira PL, Couillaud F, et al. (2013) Quantitative Evaluation of Ultrasound-Mediated Cellular Uptake of a Fluorescent Model Drug. Mol. Imaging Biol. 15:523-533.

[27] Wang JF, Wu CJ, Zhang CM, Qiu QY, and Zheng M (2009) Ultrasound-mediated microbubble destruction facilitates gene transfection in rat C6 glioma cells. Mol Rep Biol. 36:1263–1267.

[28] Liu HL, Hua MY, Chen PY, Chu PC, Pan CH, et al. (2010) Blood-brain barrier disruption with focused ultrasound enhances delivery of chemotherapeutic drugs for glioblastoma treatment. Radiology 255:415–425.

[29] Burke CW, Klibanov AL, Sheehan JP, and Price RJ (2011) Inhibition of glioma growth by microbubble activation in a subcutaneous model using low duty cycle ultrasound without significant heating. J. Neurosurg. 114:1654–1661.

[30] Ivanov AI (2008) Pharmacological Inhibition of Endocytic Pathways: Is It Specific Enough to Be Useful?, In Exocytosis and Endocytosis. Methods in Molecular Biology, Humana Press, New York 15–33.

[31] Thors L, Alajakku K and Fowler CJ (2007) The ‘specific’ tyrosine kinase inhibitor genistein inhibits the enzymic hydrolysis of anandamide: implications for anandamide uptake. Br. J. Pharmacol. 150:951–960.

[32] Vercauteren D, Vandenbroucke RE, Jones AT, Rejman J, Demeester J, et al. (2010) The Use of Inhibitors to Study Endocytic Pathways of Gene Carriers: Optimization and Pitfalls. Mol. Ther. 18:561–569.

[33] Roth BL, Poot M, Yue ST and Millard PJ (1997) Bacterial viability and antibiotic susceptibility testing with SYTOX green nucleic acid stain. Appl. Environ. Microbiol. 63:2421–2431.

[34] Deckers R, Yudina A, Cardoit LC and Moonen C (2011). A fluorescent chromophore TOTO 3 as a 'smart probe' for the assessment of ultrasound mediated local drug delivery in vivo. Contrast Media Mol. Imaging 6:267–274.

[35] Lammertink B, Deckers R, Storm G, Moonen C, and Bos C (2015) Duration of ultrasound-mediated enhanced plasma membrane permeability. Int. J. Pharm. 482:92-98.

[36] Escoffre JM, Novell A, Piron J, Zeghimi A, Doinikov A et al. (2013) Microbubble attenuation and destruction: are they involved in sonoporation efficiency?. IEEE Trans. Ultrason., Ferroelectr. Freq. Control. 60:46-52

[37] Loy G, Zelinsky A (2003) Fast radial symmetry for detecting points of interest. IEEE Trans. Pattern Anal. 25:959–973.

[38] Horowitz SB (1972) The Permeability of the Amphibian Oocyte Nucleus in Situ. J. Cell Biol. 54:609-625.

[39] Gerace L and Burke B (1988) Functional organization of the nuclear envelope. Ann. Rev. Cell Biol. 4:335–374.

[40] Oropesa-Ávila M, Fernández-Vega A, de la Mata M, Maraver JG, Cordero MD, et al. (2013) Apoptotic microtubules delimit an active caspase free area in the cellular cortex during the execution phase of apoptosis. Cell Death Dis. 4:e527.

[41] Yudina A, Lepetit-Coiffé M, Moonen C (2011) Evaluation of the Temporal Window for Drug Delivery Following Ultrasound-Mediated Membrane Permeability Enhancement. Mol. Imaging Biol. 13:239–249.

Supplementary materials

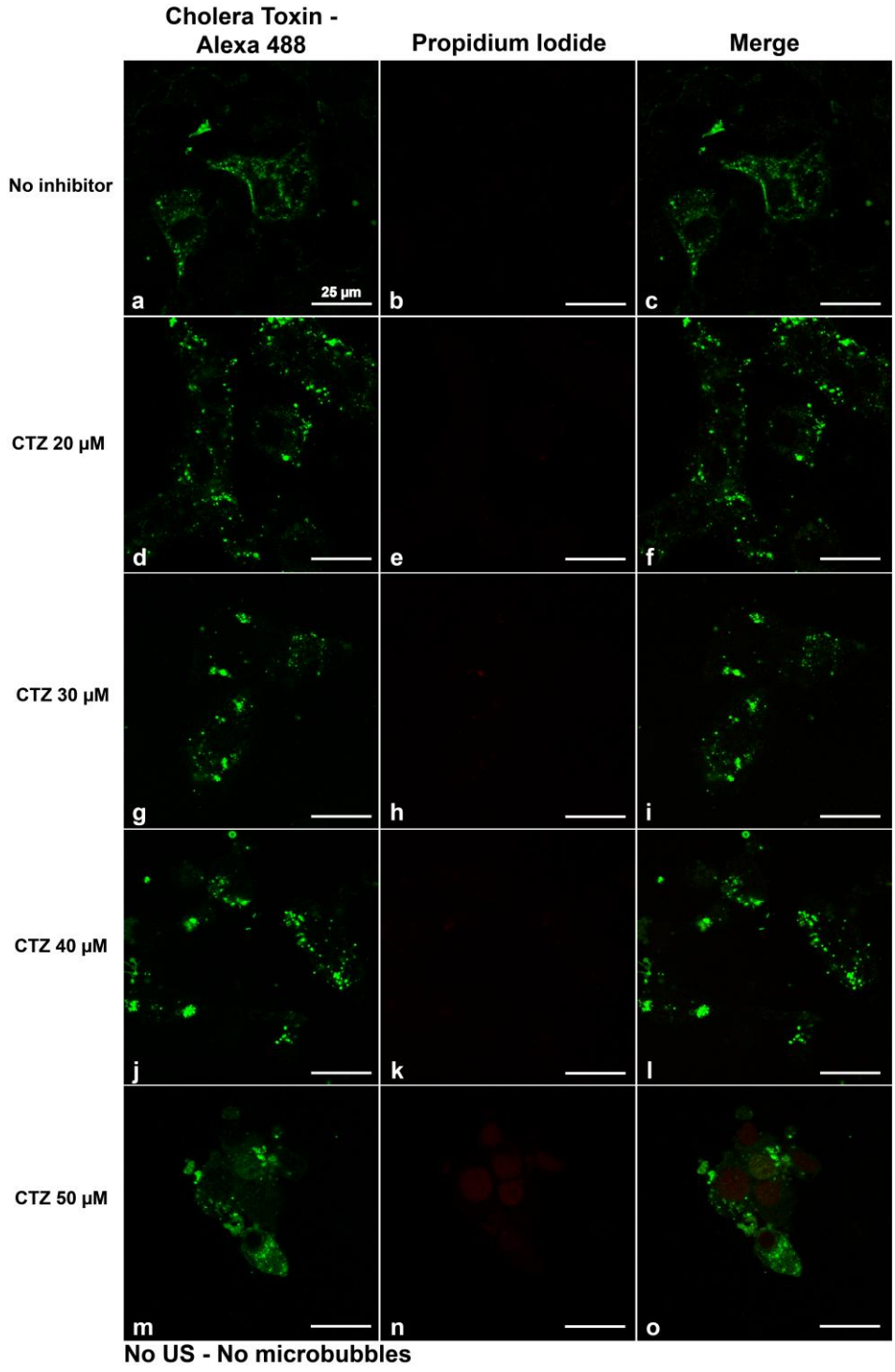

Figure S1. Specificity experiment – Effect of chlorpromazine (CTZ) from 0 µM to 50 µM on caveolae vesicles (green channel: Cholera Toxin – Alexa Fluor 488 nm conjugate) (a,d,g,j,m). Cell plasma membrane integrity is evaluated using Propidium Iodide (PI – red channel) (b,e,h,k,n). Bar: 25 µm.

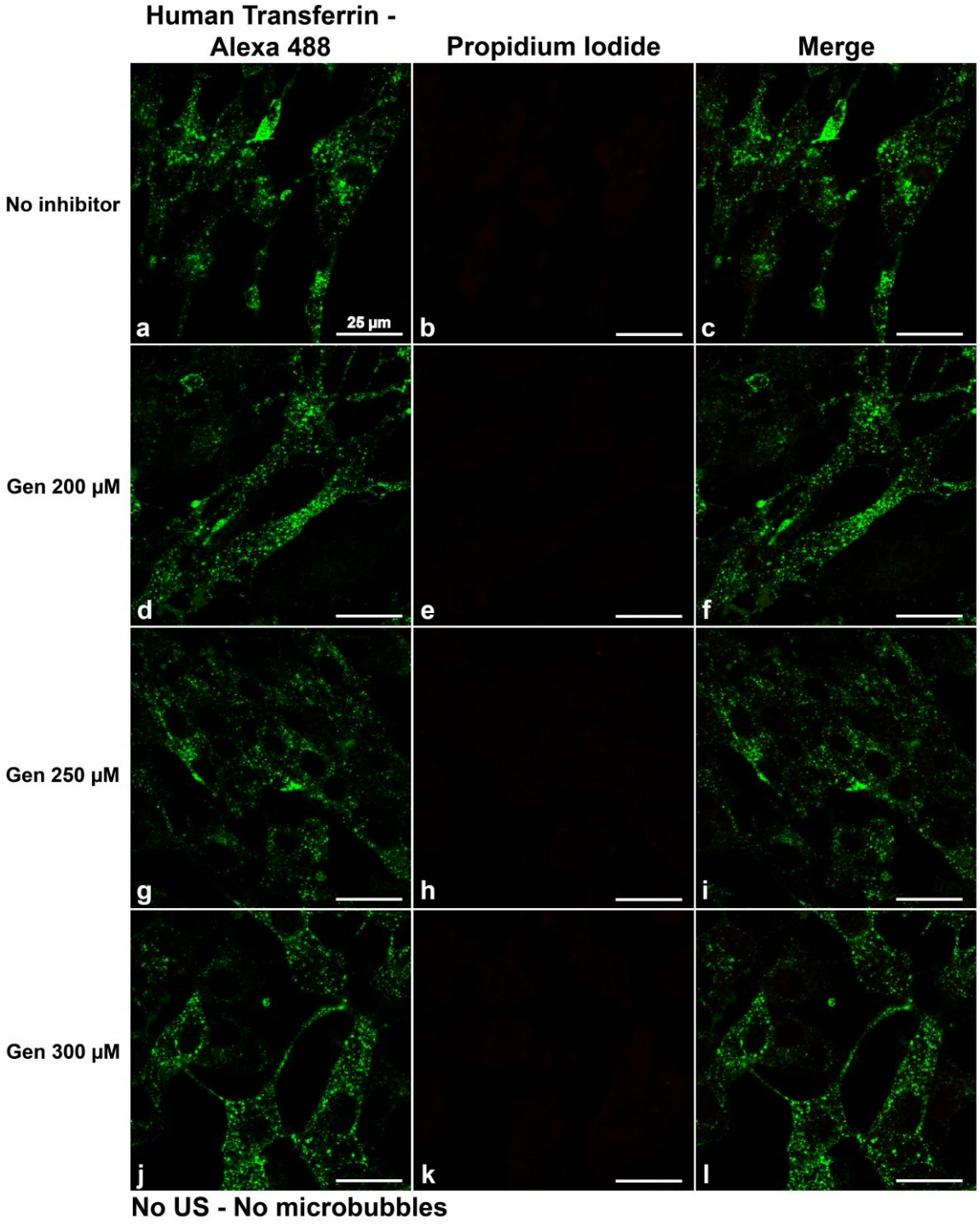

Figure S2. Specificity experiment – Effect of genistein (Gen) from 0 µM to 300 µM on clathrin vesicles (green channel: Human Transferrin – Alexa Fluor 488 nm conjugate) (a,d,g,j). Cell plasma membrane integrity is evaluated using Propidium Iodide (PI – red channel) (b,e,h,k). Bar: 25 µm.

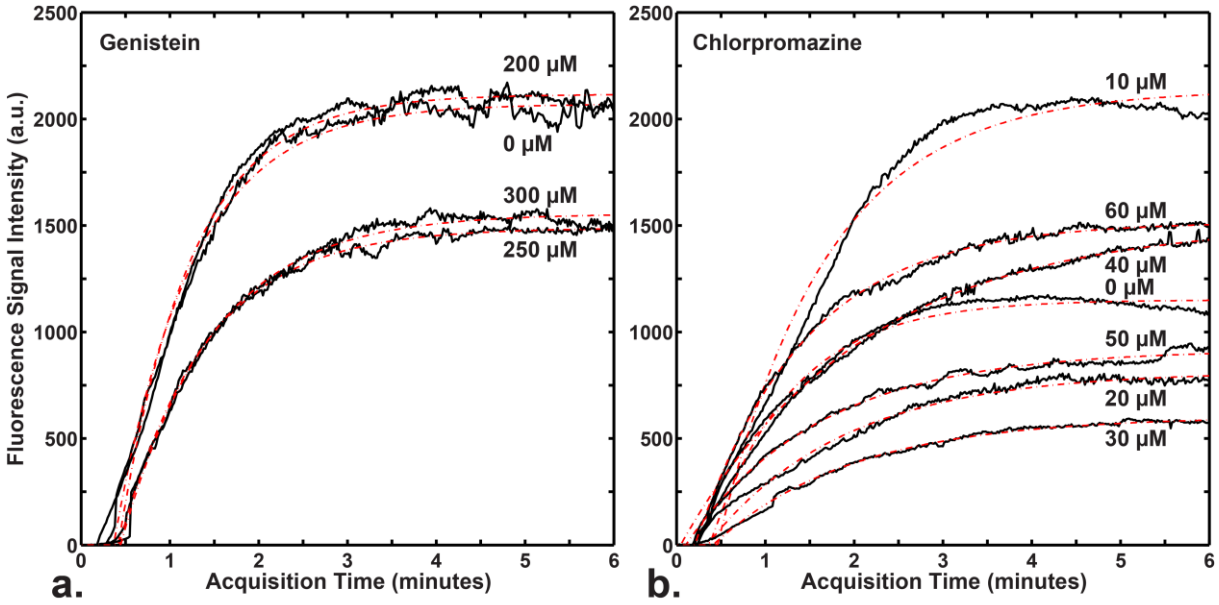

	Concentration (µM)	1/k	r^2
genistein	0	52 s	0.987
	200	49 s	0.988
	250	58 s	0.996
	300	1 min 1 s	0.992
chlorpromazine	0	56 s	0.979
	10	1 min 23 s	0.976
	20	1 min 32 s	0.983
	30	1 min 34 s	0.992
	40	2 min 2 s	0.998
	50	1 min 31 s	0.991
	60	1 min 14 s	0.997

c.

Figure S3. Examples of fluorescence signal profiles of the uptake of cells in presence of genistein from 0 to 300 µM (a), and chlorpromazine from 0 to 60 µM (b). Using a two-compartment model, the curve obtained by the fitting procedure for one cell (red dashed line) is superimposed to the experimental signal intensity profile (dark plain line). For each condition, the uptake time constant 1/k derived from the signal profile in b by the fitting procedure are shown in table c. (r^2: Pearson's correlation coefficient of the fit).